

Ellipsometric studies of electronic interband transitions in $\text{Cd}_x\text{Hg}_{1-x}\text{Te}$

L. Viña, C. Umbach,* M. Cardona, and L. Vodopyanov,[†]

Max-Planck-Institut für Festkörperforschung, Heisenbergstrasse 1, D-7000 Stuttgart 80, Federal Republic of Germany

(Received 21 February 1984)

Ellipsometric measurements of the dielectric constant of $\text{Cd}_x\text{Hg}_{1-x}\text{Te}$ alloys were performed at room temperature between 1.8 and 5.5 eV for samples covering the whole range of concentrations. The dependence of the E_1 , $E_1 + \Delta_1$, and E_2 threshold energies on x was obtained: It is quadratic for E_1 and $E_1 + \Delta_1$ and linear within experimental error for E_2 . An upwards bowing is found for the spin-orbit splitting Δ_1 as a function of x . The effect of alloying in broadening the observed structures is relatively small. However, a large decrease of excitonic effects in the E_1 and $E_1 + \Delta_1$ gaps due to alloying has been observed. These results are discussed in the light of recent coherent-potential-approximation calculations.

I. INTRODUCTION

$\text{Cd}_x\text{Hg}_{1-x}\text{Te}$ substitutional pseudobinary alloys are a mixture of a semimetal (HgTe) with a semiconductor (CdTe), crystallizing in the zinc-blende structure. The lattice parameters of the parent compounds are nearly the same ($\Delta a/a = 0.003$). The fundamental energy gap E_0 varies with composition continuously from -0.3 eV (for HgTe) to 1.6 eV (for CdTe).^{1,2} Considerable attention has been devoted in the last years to these alloys due to their applications as infrared detectors (for a recent review, see Ref. 3). The study of the optical properties of semiconducting alloys is very useful in analyzing band-structure changes from one semiconductor to another. The properties at energies greater than those of the fundamental gap E_0 are of interest since the structure in the optical spectra can be assigned to direct electronic interband transitions at specific regions of the Brillouin zone (BZ) and therefore can be related to the band structure of the semiconductor alloys.

The change in the fundamental gap of $\text{Cd}_x\text{Hg}_{1-x}\text{Te}$ with composition has been investigated mainly with optical methods such as absorption⁴⁻¹¹ and reflection spectroscopy.¹²⁻²⁰ The latter technique, together with modulation methods,²¹⁻²⁶ has been employed to study higher edges above the fundamental one. Ellipsometry measurements have been performed on HgTe,^{27,28} CdTe,^{28,29} and $\text{Cd}_{0.29}\text{Hg}_{0.71}\text{Te}$.²⁸ Heterojunctions of HgTe/CdTe have also been the object of investigations.³⁰⁻³² Band-structure calculations are available for the parent compounds³³⁻³⁹ and the mixed crystals.⁴⁰⁻⁴⁹ The main effect that alloying has on the fundamental gap is the quadratic dependence of the energy thresholds on composition x ; early experimental evidence of this dependence was found in the alloys of the cuprous halides.⁵⁰ The bowing can be separated in two contributions:⁵¹ Intrinsic bowing due to differences in the lattice constant between the various compounds arises in the virtual-crystal approximation mainly from the averaging and renormalization procedures of the two constituent potentials that account for modification of screening and scaling with lattice constant. This intrinsic effect is always found to be smaller

than the experimental one, especially in the case of $\text{Cd}_x\text{Hg}_{1-x}\text{Te}$ and is expected to be small because of the very small change in lattice parameter with x . Extrinsic bowing—the difference between intrinsic and experimental bowing—is attributed to the effects of the random potential due to disorder.

For higher gaps the magnitude and even the sign of the bowing relative to the fundamental edge can change, as has been suggested by Stroud.⁵² Lifetime broadening effects due to alloying are also present in higher gaps.⁴⁸ Another effect which is mainly disorder induced is the nonlinear dependence of spin-orbit (SO) splitting on alloy composition.^{53,54}

A discrepancy is found in the literature concerning the effect of bromine-methanol etching on $\text{Cd}_x\text{Hg}_{1-x}\text{Te}$ alloys. Electroreflectance (ER),²⁶ x-ray photoemission spectroscopy (XPS),⁵⁵ and Auger-electron spectroscopy (AES)⁵⁶ measurements show the presence of a damaged, Te-rich layer after the etching treatment. Ellipsometry²⁸ measurements for $\text{Cd}_{0.29}\text{Hg}_{0.71}\text{Te}$, however, indicate no evidence of such a layer.

In this work we present an ellipsometric study at room temperature of the $\text{Cd}_x\text{Hg}_{1-x}\text{Te}$ alloys ($0 \leq x \leq 1$) in the energy range from the near infrared (1.8 eV) to the near ultraviolet (5.5 eV). The ellipsometric method has been shown to be particularly suitable for the investigation of interband transitions and the corresponding critical points.^{57,58} We study the higher interband transitions labeled E_1 , $E_1 + \Delta_1$, and E_2 . The E_1 and $E_1 + \Delta_1$ edges are due to transitions along the Λ direction in the BZ, between the $\Lambda_{4,5}$ valence band and the Λ_6 conduction band for E_1 and between the Λ_6 valence band and the Λ_6 conduction band for the SO-split $E_1 + \Delta_1$. The E_2 transition takes place in an extended region of \vec{k} space close to the X point combined with regions near the $\{110\}$ and $\{100\}$ directions. The points (0.75,0.75,0), (0.14,0,0), and (0.8,0.2,0.2) have been assigned³⁹ to the E_2 transition in HgTe; the corresponding points in the case of CdTe are³⁹ (0.7,0.7,0), (0.7,0,0), and (0.9,0.2,0.2). An accurate determination of the energy threshold (E), broadening (Γ), and phase (ϕ) of the critical point (cp) is obtained through analysis of numerical second derivative spectra of the

complex dielectric constant with respect to the photon energy, $d^2\epsilon/d\omega^2$. The line-shape analysis of the ellipsometric data by fitting with analytical expressions the derivative spectra avoids the arbitrariness of assigning the peak position of reflectivity to the cp energy and the ambiguities present in the interpretation of ER spectra due to the complex prefactors that appear in the expression of their line shape.⁵⁹ A two-dimensional saddle point with some admixture of a maximum was used to fit the E_1 and $E_1 + \Delta_1$ cp and a one-dimensional maximum for E_2 . The admixture of saddle point and maximum results from excitonic interactions and is shown to reach its maximum in the case of CdTe.

We found a quadratic dependence of the E_1 and $E_1 + \Delta_1$ cp on composition x with the bowing parameters $c(E_1) = 0.7 \pm 0.1$, $c(E_1 + \Delta_1) = 0.6 \pm 0.1$, and, within the experimental accuracy, a linear dependence of E_2 ; the bowing parameter extracted from the fit was in this case $c(E_2) = 0.06 \pm 0.08$. An increase of the Lorentzian broadening parameter of the alloys with respect to the parent compounds was observed for E_1 and $E_1 + \Delta_1$, reaching its maximum at a concentration of about $x = 0.8$. However, we found a decrease of Γ for the E_2 structure of the alloys with a minimum at a concentration $x \sim 0.7$. Owing to the relatively complicated dependence of ϕ on x we did not attempt to fit it to any analytical expression.

The paper is organized as follows: experimental details are described in Sec. II. The results are presented in Sec. III and discussed in Sec. IV.

II. EXPERIMENTAL

Ten $\text{Cd}_x\text{Hg}_{1-x}\text{Te}$ crystals with composition between $x = 0$ and 1 were used to prepare samples. The crystals were grown in tellurium solvent from earlier synthesized CdTe and HgTe with a special traveling heater crystallization method.⁶⁰ The homogeneity of the samples was controlled by x-ray microprobe analysis⁶¹ and by ellipsometric measurements at different positions across the surface. The surfaces to be measured were mechanically polished with Syton, followed by a chemomechanical polishing with a bromine-methanol solution.

Room-temperature pseudodielectric functions $\epsilon(\omega) = \epsilon_1(\omega) + i\epsilon_2(\omega)$ were obtained with an automatic rotating analyzer ellipsometer of the type developed by Aspnes⁶² and described elsewhere.⁵⁸ The samples were mounted and optically aligned with a He-Ne laser in a windowless cell in flowing dry N_2 to minimize surface contamination. They were etched *in situ* prior to measurement with different bromine-methanol solutions²⁸ and stripped with methanol and distilled water; real-time ellipsometric measurements at the energy of the E_2 peak were taken simultaneously. The treatment was repeated using the criterium of obtaining the largest value of ϵ_2 at this photon energy.⁶³ This situation should represent the most abrupt mismatch of optical constants between bulk and ambient and allow us to use the two-phase model⁶⁴ to obtain ϵ . The best results were obtained with a 0.01 vol. % bromine in methanol mixture. The spectra were measured immediately after etching in a cell flushed with dry nitrogen at an angle of incidence of 67.5° .

III. RESULTS

In Fig. 1 we show the optical constants of a $\text{Cd}_{0.29}\text{Hg}_{0.71}\text{Te}$ sample obtained in the present work (solid curves) together with measurements of a sample with equal nominal composition obtained from Ref. 28 (dotted-dashed lines). The main discrepancy, 0.5 units in ϵ_2 at E_2 , is due, we believe, to the different etching procedures used; we did not employ the $\text{HNO}_3:\text{H}_2\text{O}$ and $\text{HCl}:\text{H}_2\text{O}$ mixtures to avoid possible formation of a Terich layer.²⁸ The difference of 0.5 is just the same found in Fig. 5a of Ref. 28 before using the $\text{HCl}:\text{H}_2\text{O}$ solution. The energy positions of the peaks are seen to be in good agreement. The presence of a damaged surface layer depleted in Te as large as 600 \AA ,²⁶ due to the bromine-methanol treatment, would result in a much larger discrepancy in the ϵ_2 values at E_2 compared with that of Ref. 28 ($\sim 4.6 \text{ eV}$ for $\text{Cd}_{0.29}\text{Hg}_{0.71}\text{Te}$) and in an increase in the broadening parameters.²⁶ In Ref. 26, after one anodization step, a broadening parameter for the E_1 transition $\sim 200 \text{ meV}$ is reported; this decreases to a value $\sim 150 \text{ meV}$ after three steps; our values for the broadening of E_1 are for all compositions below 150 meV (see Fig. 7) indicating that such a damage did not happen after the chemical processing. Our results confirm the fact found in Ref. 28 that no evidence for such a layer is seen with ellipsometry.

The real and imaginary part of the pseudodielectric constant (ϵ) for HgTe, CdTe, and five selected compositions ($x = 0.2, 0.43, 0.76, 0.86, \text{ and } 0.91$) are shown in Figs. 2 and 3, respectively. A two-phase model⁶⁴ in which the surface is treated as a simple plane boundary between

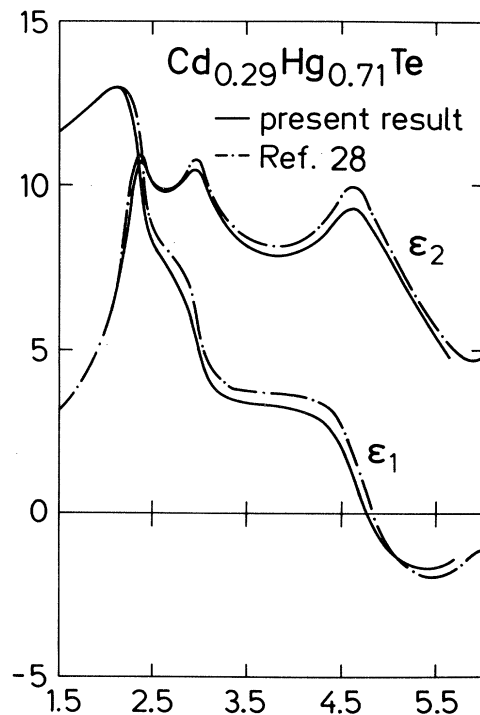


FIG. 1. Solid curves: real (ϵ_1) and imaginary (ϵ_2) part of the pseudodielectric constant of $\text{Cd}_{0.29}\text{Hg}_{0.71}\text{Te}$ at room temperature. Dotted-dashed curves: real and imaginary part of a sample of equal nominal composition taken from Ref. 28.

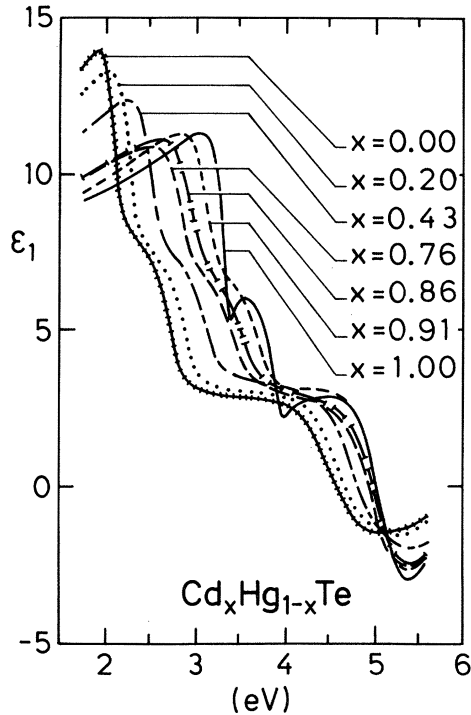


FIG. 2. Real part (ϵ_1) of the pseudodielectric constant of HgTe ; \cdots , $\text{Cd}_{0.20}\text{Hg}_{0.80}\text{Te}$; $-\cdot-, $\text{Cd}_{0.43}\text{Hg}_{0.57}\text{Te}$; $---$, $\text{Cd}_{0.76}\text{Hg}_{0.24}\text{Te}$; ---|---| , $\text{Cd}_{0.86}\text{Hg}_{0.14}\text{Te}$; $---$, $\text{Cd}_{0.91}\text{Hg}_{0.09}\text{Te}$, and $---$, CdTe (room temperature).$

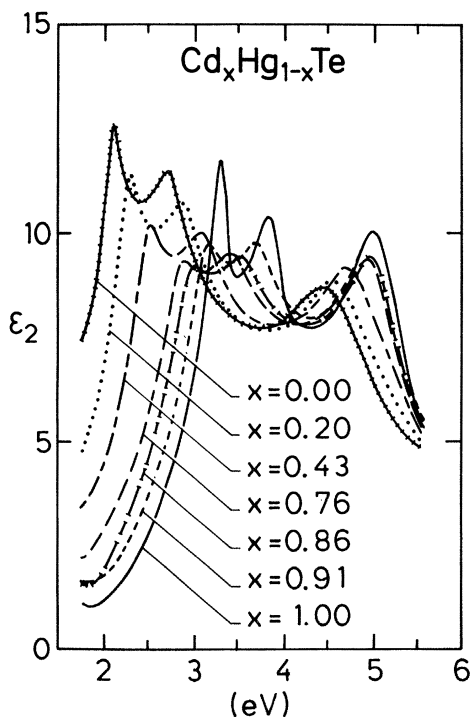


FIG. 3. Imaginary part (ϵ_2) of the pseudodielectric constant of HgTe , CdTe , and $\text{Cd}_x\text{Hg}_{1-x}\text{Te}$ with $x=0.20, 0.43, 0.76, 0.86,$ and 0.91 (room temperature). The symbols are the same as in Fig. 2.

two homogeneous media was used to obtain these spectra from the measured complex reflectance ratios. The optical activity⁶⁵ of the quartz Rochon prisms was also taken into account in the treatment of the data. The most important fact in these figures is the shift of the three main peaks (E_1 , $E_1 + \Delta_1$, and E_2) to higher energies with increasing composition x . A small shoulder corresponding to the $E_0 + \Delta_0$ cp at ~ 2.5 eV is also seen in the case of CdTe . A decrease of the magnitude of ϵ_1 at the E_1 peak happens until concentrations of ~ 0.7 , then this feature begins smoothly to increase until it reaches the corresponding value of CdTe . The same behavior is observed for ϵ_2 at the E_1 and $E_1 + \Delta_1$ structures. The excitonic effect near the E_1 and $E_1 + \Delta_1$ cp is also seen in these figures, especially in the case of CdTe :⁶⁶ the peaks in ϵ_2 are clearly asymmetric and drop more sharply on the high-energy side. The asymmetry of the spectra for compositions $x < 0.9$ resemble that observed for HgTe .

To enhance the structure present in the spectra and obtain the cp parameters we calculate numerically the second derivative spectra, $d^2\epsilon/d\omega^2$, of the complex dielectric function from our ellipsometric data. Tabulated coefficients taken from the literature⁶⁷ were used to compute the derivatives; an appropriate level of smoothing was also chosen in order to suppress the noise in the derivative spectra without distorting the line shape. Typical results for $d^2\epsilon_1/d\omega^2$ and $d^2\epsilon_2/d\omega^2$ of the E_1 and $E_1 + \Delta_1$ transitions are shown in Fig. 4 for CdTe (dashed lines), HgTe (solid lines), and $\text{Cd}_{0.43}\text{Hg}_{0.57}\text{Te}$ (dotted-dashed lines, the spectra of HgTe and $\text{Cd}_{0.43}\text{Hg}_{0.57}\text{Te}$ are enlarged by factors of 1.5 and 4, respectively). The derivative spectra were fitted assuming a two-dimensional saddle point for the E_1 and $E_1 + \Delta_1$ singularities and a one-dimensional maximum for the E_2 cp. A least-squares procedure using the Marquardt method⁶⁸ was used for the fit, with both the real and the imaginary parts of $d^2\epsilon/d\omega^2$ fitted simultaneously. Excitonic effects were also taken into account in a standard way by allowing a mixture of two cp.^{59,69,70}

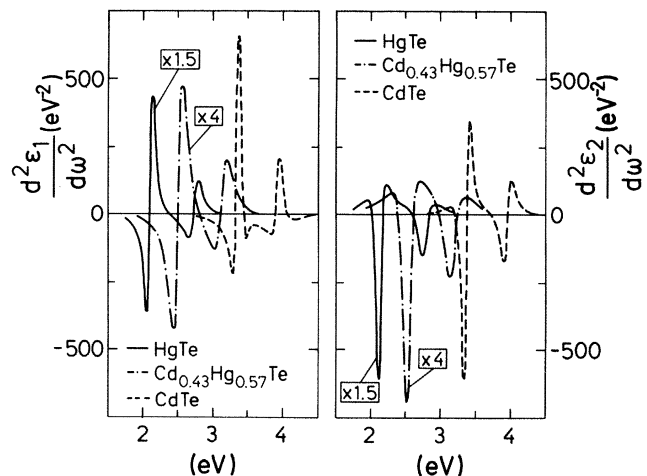


FIG. 4. Second derivatives with respect to the photon energy of the real ($d^2\epsilon_1/d\omega^2$) and imaginary ($d^2\epsilon_2/d\omega^2$) part of the pseudodielectric function of HgTe ; $---$, $\text{Cd}_{0.43}\text{Hg}_{0.57}\text{Te}$, and $---$, CdTe . The derivative spectra of HgTe and $\text{Cd}_{0.43}\text{Hg}_{0.57}\text{Te}$ are enlarged by factors of 1.5 and 4, respectively.

Hence a two-dimensional saddle point and a maximum, which was found to give the best fit, were used for the E_1 and $E_1 + \Delta_1$ data, and both singularities were fitted simultaneously. The mixture of contiguous two-dimensional cp can be represented by^{59,69,70}

$$\epsilon \sim A - i \ln(\omega_0 - \omega - i\Gamma) e^{i\phi}, \quad (1)$$

where the angle represents the amount of mixture. We present in Fig. 5 the values of ϕ versus composition x obtained from our fits for E_1 (dots) and $E_1 + \Delta_1$ (triangles). Four parameters were used for each E_1 and $E_1 + \Delta_1$ cp (amplitude, energy, Lorentzian broadening, and phase) and only the first three for E_2 . The large phase angles are consistent with one-electron calculations of ϵ_2 in zinc-blende materials which underestimate strength of E_1 and $E_1 + \Delta_1$ structures and with ER measurements in Ge.⁷¹

Figure 6 shows the energy position of the E_1 , $E_1 + \Delta_1$, E_2 and Δ_1 (obtained by subtraction of E_1 from $E_1 + \Delta_1$) as a function of x . The E_1 structure corresponds to transitions from the $\Lambda_{4,5}$ valence band to the Λ_6 conduction band, $E_1 + \Delta_1$ (black dots) to transitions from the Λ_6 valence band to the Λ_6 conduction band, and E_2 to transitions in an extended region of the BZ.³⁹ The open circles are data taken from ER measurements by Moritani *et al.*²⁴ and are included for comparison. The results show a quadratic dependence of the gaps on concentration as in many other semiconducting mixed crystals.^{50,54,57,72-77} The solid lines correspond to the best fit of our data to the expression,

$$E(x) = a + bx + cx^2. \quad (2)$$

The values of a , b , and c for the three structures, as well as the SO splitting, are listed in Table I with the corresponding uncertainties representing 90% reliability. In

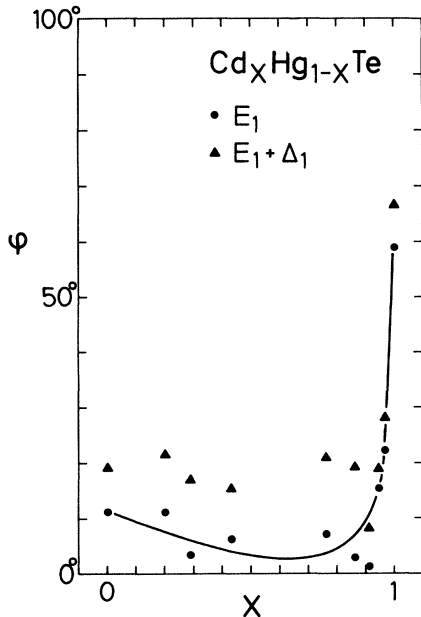


FIG. 5. Dependence on composition (x) of the excitonic parameter ϕ , defined in Eq. (1) for the E_1 (dots) and $E_1 + \Delta_1$ (triangles) critical points. The solid line is displayed as a guide to the eye.

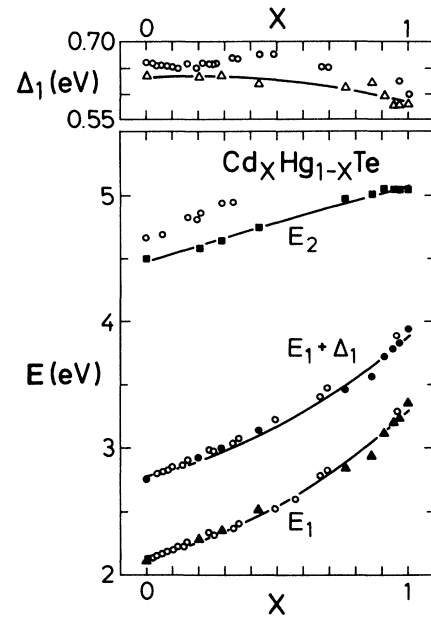


FIG. 6. Dependence on composition of critical-point energies and spin-orbit splitting of $\text{Cd}_x\text{Hg}_{1-x}\text{Te}$. Black triangles: E_1 critical point. Black dots: $E_1 + \Delta_1$ critical point. Squares: E_2 critical point. Open triangles: spin-orbit splitting (Δ_1). The open circles are electoreflectance data taken from Ref. 24. Solid lines represent the best fits of our data to a quadratic function [$E(x) = a + bx + cx^2$].

this table the values of the parameters obtained from reflection^{17,19} and ER measurements²⁴ are also presented. A negative value for the bowing parameter ($c = -0.079$) of the SO splitting (Δ_1) in $\text{Cd}_x\text{Hg}_{1-x}\text{Te}$ is also found in III-V (Refs. 54, 75, 76, and 78-80) and quaternary^{57,77,81-83} alloys.

The Lorentzian broadening parameters Γ for the E_1 (triangles), $E_1 + \Delta_1$ (squares), and E_2 (dots) cp are displayed in Fig. 7. Lines are drawn through the experimental points only to visualize the dependence on concentration. The three structures are seen to be broader in HgTe than in CdTe by a factor 1.15 for E_1 , 1.3 for $E_1 + \Delta_1$, and 1.6 for E_2 . The broadening of the $E_1 + \Delta_1$ cp is also always larger than that of the E_1 structure, this happens also in the case of Ge,⁷¹ $(\text{Ga}_{1-x}\text{Al}_x)_{0.47}\text{In}_{0.53}\text{As}$,⁸³ and $\text{In}_{1-x}\text{Ga}_x\text{As}_y\text{P}_{1-y}$.⁵⁷ Our value of $\Gamma = 65$ meV for E_1 in CdTe (at room temperature) is in good agreement with thermoreflectance measurements of CdTe (Ref. 84) where $\Gamma = 49.3$ meV (at 203 K) and $\Gamma = 88.4$ meV (at 324 K) are found by fitting the spectra with derivatives of an asymmetric Lorentzian line. An asymmetric composition dependence of the broadening is found; it peaks at a composition between $x = 0.7$ and 0.8 . Reflection measurements⁸⁵ of excitonic structures close to the fundamental gap in $\text{CdS}_{1-x}\text{Te}_x$, $\text{CdS}_{1-x}\text{Se}_x$, and $\text{Zn}_x\text{Cd}_{1-x}\text{S}$ also show an asymmetric x dependence for the broadening of the exciton line. Our results give an increase of Γ for E_1 and $E_1 + \Delta_1$ in the mixed crystals with respect to the parent compounds; however, a decrease in the broadening for the alloys in comparison with HgTe and CdTe is seen for the E_2 structure.

TABLE I. Values of the parameters a , b , and c obtained by fitting the critical-point energy (E) vs composition (x) to the equation, $E = a + bx + cx^2$. All values correspond to room temperature.

Critical point	a (eV)	b (eV)	c (eV)
E_1	2.147 ± 0.005^a	0.44 ± 0.02^a	0.7 ± 0.1^a
	2.11^b	0.31^b	0.87^b
	2.15^c	0.35^c	0.86^c
	2.068^d	1.42^d	-3.5^d
$E_1 + \Delta_1$	2.778 ± 0.005^a	0.47 ± 0.02^a	0.6 ± 0.1^a
	2.74^b	0.55^b	0.6^b
	2.73^c	0.64^c	0.48^c
Δ_1	0.631 ± 0.001^a	0.031 ± 0.02^a	-0.079 ± 0.001^a
E_2	4.468 ± 0.003^a	0.66 ± 0.01^a	-0.06 ± 0.08^a

^aThis work.

^bReference 19.

^cData from Ref. 24 and fitted in Ref. 17.

^dReference 17 only in the region $0 \leq x \leq 0.16$.

^eReference 17.

IV. DISCUSSION

The agreement between the critical-point energies for the E_1 transitions found in this work and in ER measurements²⁴ is found to be good. However, the cp energies of $E_1 + \Delta_1$ (and therefore Δ_1) and E_2 from Ref. 24 are somewhat larger than the present results, especially in the case of E_2 . No attempt to analyze the line shape was made in Ref. 24, the photon energies of the dominant peaks in the ER spectra were taken as the cp energy. Our complete line-shape analysis of the derivative spectra allows us to obtain precisely the cp energies, the only uncertainty being the assignment of the type of cp. The effect of the broadening is to move the peak positions away from the true critical-point energies, the discrepancies being larger

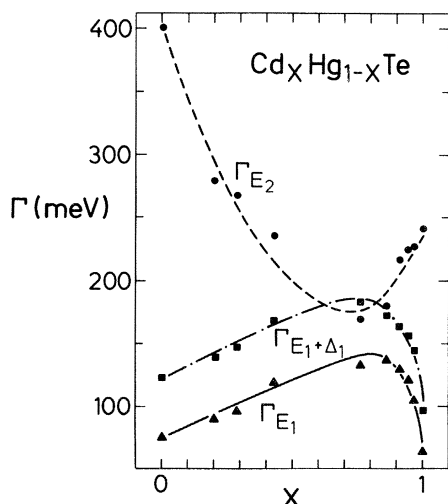


FIG. 7. Dependence of critical-point broadening parameters on composition. Triangles: broadening parameter (Γ) for the E_1 transition. Squares: Γ corresponding to $E_1 + \Delta_1$. Dots: Γ for the E_2 singularity. Lines are only displayed as a guide to the eye.

(e.g., E_2 ; see Fig. 6) in the case of structures with larger broadening parameters. Therefore, the practice of associating cp energies with peaks in ϵ_2 , reflection or modulation spectra can lead to substantial errors and should be avoided. We shall mention the existence of a method recently developed by Aspnes⁸⁶ to investigate critical points by means of Fourier analysis. This method gives very precisely cp parameters without using numerical derivative procedures which may, in some cases, distort the line shape of the structures. We plan to use it in future work.

The simplest approximation to the band structure of alloys is the virtual crystal approximation (VCA). In it the alloy potential is replaced by the average potential with the lattice periodicity. If the lattice constants of the two components are very close, as is the case for $\text{Cd}_x\text{Hg}_{1-x}\text{Te}$, the various VCA pseudopotential form factors (or other potential parameters) are linear in x . Differences in the lattice constants introduce nonlinearities in V_G versus x which should be negligible in our case. In spite of the linear dependence of the potential $V_x(\vec{r})$ on x , nonlinearities in the x dependence of the energy gaps can result when the complete Hamiltonian is solved. From the point of view of perturbation theory the simplest nonlinearities arise from the coupling of states of the same symmetry (at the same \vec{k}) by the perturbing potential $V_x - V_0$. The lower the symmetry of the BZ point, the more states of the same symmetry exist. Hence, following this argument, one would expect a smaller quadratic dependence for the E_0 gap (at Γ) with x than for the E_1 gap (Λ direction). We have performed a VCA pseudopotential calculation of the E_0 and the E_1 gaps of $\text{Hg}_{1-x}\text{Cd}_x\text{Te}$ versus x with the pseudopotentials of Chadi and Cohen.⁴³ For the E_1 we have taken an average of k points between $\vec{k} = (0.30\pi/a)(111)$ and the L point. This calculation yields for the bowing parameters C of the E_0 and E_1 gaps,

$$C(E_0) = 0.06 \pm 0.01 \text{ eV}; \quad C(E_1) = 0.28 \pm 0.02 \text{ eV}.$$

These results confirm our conjecture: the bowing parameter $C(E_0)$ of the E_0 gap at the Γ point is negligible while that of the E_1 gap at the lower symmetry Λ line is quite important. It amounts to nearly half of the measured value. The intermediate state most likely to be responsible for the VCA bowing of the E_1 and $E_1 + \Delta_1$ gaps is the second lowest Λ_1 conduction-band state interacting with the lowest Λ_1 conduction band.

Besides the VCA bowing just described there exists a bowing due to the effect of the potential fluctuations around the VCA average potential. This bowing is automatically included in the coherent-potential approximation (CPA) calculations of Ref. 48 which yield a total $C \approx 0.71$, in agreement with the experimental results (we note, however, that these calculations were performed only for the gap at the L point). In view of the discussion above we conclude that approximately half of the observed C has its origin in the virtual crystal potential while the other half is due to potential fluctuations.

Our conclusions about the near linearity of $E_0(x)$ agree with those of Refs. 43 and 40. However, they disagree with Podgórný and Czyżyk⁴⁴ who find $C(E_0) = 0.97$ eV with a tight-binding calculation in the VCA. Also, the dielectric method of Van Vechten and Bergstresser^{24,51} gives nearly the same C for E_0 as for E_1 , a fact which is not surprising since within this model all gaps have the same behavior as the average dielectric gap.⁸⁷

It has been pointed out⁵² that the potential fluctuations may lead to an upwards bowing ($C < 0$) for the highest critical points such as E_2 . This value of $C(E_2)$ found in the present work [$C(E_2) = -0.06(8)$ eV] is indeed slightly negative although it could be zero within the experimental error. A linear dependence of the E_2 gap on composition has also been found for $\text{GaAs}_x\text{P}_{1-x}$,⁷² $\text{In}_{1-x}\text{Ga}_x\text{As}_y\text{P}_{1-y}$,⁵⁷ and $\text{CdS}_{1-x}\text{Se}_x$.⁸⁸ Although we have fitted the x dependence of the E_1 and the $E_1 + \Delta_1$ gaps with the quadratic dependence of Eq. (2), a closer examination reveals that there are systematic deviations from this fit. In Fig. 8 we have plotted the difference d

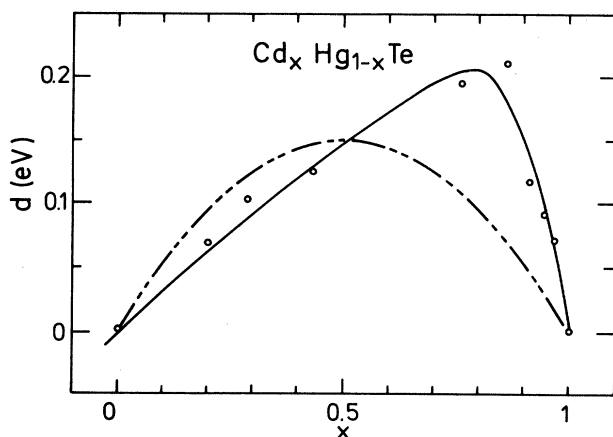


FIG. 8. Dependence on composition of the difference (d) between the experimental energy threshold values for the $E_1 + \Delta_1$ singularity and the values obtained by linear interpolation between HgTe and CdTe. The dashed line represents the parabolic result [$cx(1-x)$] with c obtained by fitting $E_1(x) + \Delta_1(x)$ to Eq. (2). The solid line is displayed as a guide to the eye.

between the observed $E_1(x)$ gaps and the linear interpolation between the E_1 gaps of CdTe and HgTe. If Eq. (2) is valid, $d(x)$ should be represented by the parabola $Cx(1-x)$, symmetric with respect to $x = 0.5$. Figure 8 shows that this is not the case, the gap is reduced by the disorder much more effectively in the CdTe-rich than in the HgTe-rich side. A similar, although smaller asymmetry has also been found for the E_1 gap of $\text{InAs}_x\text{Sb}_{1-x}$ (Ref. 78) and in a recent pseudopotential calculation⁴⁹ of the E_0 gap of $\text{Cd}_x\text{Hg}_{1-x}\text{Te}$ (in this case it is easy to explain it is due to the band crossing).

We cannot give a convincing explanation of the asymmetry of the experimental curve in Fig. 8. We note, however, that the phase angle of Fig. 5, qualitatively representative of excitonic effects, also shows an asymmetric behavior with a minimum near the maximum of Fig. 8. Similarly, the broadening parameters of Fig. 7 also show asymmetric dependence on x . The asymmetry present in the broadenings of E_1 and $E_1 + \Delta_1$ versus x (Fig. 7) can be explained qualitatively on the basis of the CPA calculations shown in Fig. 2 of Ref. 48. This figure shows that the conduction band along Λ is broadened about 3 times more efficiently by the disorder on the CdTe than on the HgTe side of the composition range, a fact which suffices to account for the asymmetric dependence of Γ_{E_1} and $\Gamma_{E_1 + \Delta_1}$ shown in Fig. 7. However, we have not been able to visualize the physical reason for this asymmetric dependence. One possibility is the fact that in the CdTe-rich end the final state for the E_1 transitions falls in an energy region where HgTe also has a large density of states. The opposite is true for the HgTe-rich end (see Fig. 3 of Ref. 48). A more detailed analysis of the calculations of Ref. 48 is necessary in order to clarify this point.

More surprising than the asymmetric behavior just discussed is the fact that the broadening parameter of the E_2 gap Γ_{E_2} exhibits a minimum for $x \approx 0.6$ (Fig. 7), a concentration close to that for which Γ_{E_1} and $\Gamma_{E_1 + \Delta_1}$ have maxima. We believe that these two facts (minimum in Γ_{E_2} and maxima in $\Gamma_{E_1}, \Gamma_{E_1 + \Delta_1}$) may be unrelated events. The E_2 transitions encompass a large region of k space including probably several critical points. If two or more of these critical points would cross in energy as a function of x the total effective width of the E_2 transitions, as obtained with a fit to a single critical point, may exhibit a minimum as a function of x . Detailed calculations of the optical combined density of states in the VCA for several values of x would be required to test this conjecture.

Owing to the strong dependence of the E_2 peak on surface characteristics,⁸⁹ it could be argued that the broadening of the E_2 singularity is, to some extent, determined by different characteristics of the surface with changing composition. Actually Γ is expected to be larger the worse the sample surface is. It is known^{19,60} that the difficulty in preparation of homogeneous $\text{Cd}_x\text{Hg}_{1-x}\text{Te}$ crystals increases with the amount of Cd; therefore, such surface effects would give a larger in the Cd-rich side, just the opposite of the experimental results. In ER measurements of Si-Ge alloys,⁹⁰ for which a line-shape analysis of the E_2 transition has been reported, an increase of Γ from

the pure materials towards the center of the compositional range is found.

The E_1 and $E_1 + \Delta_1$ transitions of tetrahedral semiconductors are known to be strongly affected by excitonic effects, i.e., electron-hole Coulomb interaction. Theoretical calculations of the effect of exciton interaction on the optical constants have been performed for diamond,⁹¹ silicon,^{92,93} and GaP.⁹⁴ This work has been reviewed in Ref. 95. These effects have also been investigated in Refs. 22, 29, 58, 59, 66, 69, 71, 84, and 96–104. A sharp drop-off of $\epsilon_2(\omega)$ above E_1 and also above $E_1 + \Delta_1$ is the most characteristic result of these effects. It has been described as the interference of a discrete two-dimensional exciton with a quasicontinuous background.⁹⁹ A simple qualitative description of these effects can be effected by multiplying the one-electron dielectric constant by a phase factor $e^{i\phi}$. We have left as an adjustable parameter in our fitting procedure.

An interesting feature of the fitted dependence is its rapid decrease for $x \leq 1$ (Fig. 5). The angle ϕ , as chosen by us, represents the amount of two-dimensional maximum added to a two-dimensional saddle point for the fit of the measured line shapes. Actually, the calculated critical point in the absence of exciton correlation should be a two-dimensional *minimum* ($\phi = -90^\circ$). Hence, we conclude from Fig. 5 that exciton effects are present for all x , becoming very strong near $x \simeq 1$. A decrease in exciton interaction would be expected as x decreases because of the increasing metalization of the compounds (increased screening). This consideration, however, cannot explain the strong decrease for $x \simeq 1$ which is possibly related to the strong increase in Γ_{E_1} and $\Gamma_{E_1 + \Delta_1}$ observed in Fig. 7 in the same region of x .

We finally discuss the dependence of Δ_1 on x shown in Fig. 6. This dependence indicates a slight upwards bowing which corresponds to $C(\Delta_1) = -0.079(1)$ eV (Table I). Similar results have been observed for the Δ_1 spin-orbit splittings of several III-V semiconductors.⁸⁰ The bowing of the Δ_0 splitting, however, is usually downwards [$C(\Delta_0) > 0$].^{80,105} The downwards bowing of Δ_0 has been interpreted as due to disorder-induced s admixture in the

Γ_{15} valence band: the s wave functions do not contribute to the spin-orbit splitting. The negative C has been attributed⁸⁰ to a repulsion between the $\Lambda_{4,5}$ and the Λ_6 valence bands due to the lowering of the local symmetry produced by the disorder. No quantitative calculation of $C(\Delta_1)$ has been performed.

V. CONCLUSIONS

Dielectric function data for the $\text{Cd}_x\text{Hg}_{1-x}\text{Te}$ alloys at room temperature in the whole range $0 \leq x \leq 1$ have been presented. The critical point energies of the three structures E_1 , $E_1 + \Delta_1$, and E_2 have been found by analysis of the numerically obtained second derivatives of the original spectra. The E_1 and $E_1 + \Delta_1$ cp have a positive bowing parameter c while the dependence of E_2 is linear within experimental accuracy. Broadening parameters and phase angles were also obtained from the line-shape analysis. A large smearing out of the excitonic effects of the E_1 and $E_1 + \Delta_1$ gaps in CdTe was found even for small Hg concentrations. The effect of alloy disorder in the E_2 gap was found to be small, possibly absent. Our results confirm previous ellipsometric data which yield no evidence of defects or disorder due to bromine-methanol etching.

Note added in proof. H. Arwin and D. E. Aspnes [J. Vac. Sci. Technol. (to be published)] have recently separated the E_2 structure of HgTe and several $\text{Cd}_x\text{Hg}_{1-x}\text{Te}$ alloys into contributions of four critical points. The separation of these critical points decreases with increasing x , a fact which may account for the Γ_{E_2} of Fig. 7.

ACKNOWLEDGMENTS

We would like to thank Dr. R. Triboulet for supplying the samples used in these experiments. Thanks are also due to G. Kisela and his group at the Max-Planck-Institut (Stuttgart) for sample preparation, and to H. Bleder and H. Birkner and the electronics group for help with the construction of the ellipsometer. We would also like to thank H. Hirt, M. Siemers, and P. Wurster for expert technical help and N. E. Christensen for helpful discussions.

*Present address: Department of Applied Physics, 212 Clark Hall, Cornell University, Ithaca, New York 14853.

†Permanent address: P.N. Lebedev Physical Institute, Academy of Sciences of the U.S.S.R., Leninsky Prospect 53, 117924 Moscow, Union of the Soviet Socialist Republics.

¹S. H. Groves, R. M. Brown, and C. R. Pidgeon, Phys. Rev. **161**, 779 (1967).

²W. G. Spitzer and C. A. Mead, J. Phys. Chem. Solids **25**, 443 (1964).

³*Narrow-Gap Semiconductors*, Vol. 98 of *Springer Tracts in Modern Physics*, edited by R. Dornhaus, G. Nimtz, and B. Schlicht (Springer, Berlin, 1983).

⁴B. T. Kolomiets and A. A. Mal'kova, Fiz. Tverd. Tela (Leningrad) **5**, 1219 (1963) [Sov. Phys.—Solid State **5**, 889 (1963)].

⁵M. D. Blue, Phys. Rev. **134**, 226 (1964).

⁶R. Ludeke and W. Paul, J. Appl. Phys. **37**, 3499 (1966).

⁷M. W. Scott, J. Appl. Phys. **40**, 4077 (1969).

⁸D. N. Tufte and E. L. Stelzer, J. Appl. Phys. **40**, 4559 (1969).

⁹J. L. Schmit and E. L. Stelzer, J. Appl. Phys. **40**, 4865 (1969).

¹⁰L. A. Bovina, V. P. Meshcheryakova, V. I. Stafeev, and E. S.

Banin, Fiz. Tekh. Poluprovodn. **7**, 40 (1973) [Sov. Phys.—Semicond. **7**, 26 (1973)].

¹¹J. Chu, S. Xu, and D. Tang, Appl. Phys. Lett. **43**, 1064 (1983).

¹²M. Cardona and D. L. Greenaway, Phys. Rev. **131**, 98 (1963).

¹³W. J. Scouler and G. B. Wright, Phys. Rev. **133**, 736 (1964).

¹⁴R. R. Galazka and A. Kisiel, Phys. Status Solidi **34**, 63 (1969).

¹⁵I. M. Nesmelova, N. S. Baryshev, F. P. Volkova, and A. P. Cherkasov, Fiz. Tekh. Poluprovodn. **6**, 950 (1972) [Sov. Phys.—Semicond. **6**, 822 (1972)].

¹⁶J. L. Freeouf, Phys. Rev. B **7**, 3810 (1973).

¹⁷A. Kisiel, M. Podgórnny, A. Rodzik, and W. Giritat, Phys. Status Solidi B **71**, 457 (1975).

¹⁸A. Kisiel, M. Zimnal-Starnawska, S. H. Ignatowicz, J. M. Pawlikowski, and J. Piotrowski, Thin Solid Films **37**, L35 (1976).

¹⁹V. G. Sredin, V. G. Savitskii, Y. V. Danilyuk, M. V. Milyanch, and V. Petrovich, Fiz. Tekh. Poluprovodn. **15**, 433 (1981) [Sov. Phys.—Semicond. **15**, 249 (1981)].

²⁰S. Yamada, J. Phys. Soc. Jpn. **15**, 1940 (1960).

- ²¹M. Cardona, K. L. Shaklee, and F. H. Pollak, *Phys. Rev.* **154**, 696 (1967).
- ²²K. L. Shaklee, J. E. Rowe, and M. Cardona, *Phys. Rev.* **174**, 828 (1968).
- ²³A. Moritani, K. Taniguchi, C. Hamaguchi, J. Nakai, R. Ueda, O. Ohtsuki, and Y. Ueda, *J. Phys. Soc. Jpn.* **31**, 945 (1971).
- ²⁴A. Moritani, K. Taniguchi, C. Hamaguchi, and J. Nakai, *J. Phys. Soc. Jpn.* **34**, 79 (1973).
- ²⁵A. Moritani, C. Hamaguchi, and J. Nakai, *Surf. Sci.* **37**, 769 (1973).
- ²⁶A. Lastras-Martínez, U. Lee, J. Zehnder, and P. M. Raccah, *J. Vac. Sci. Technol.* **21**, 157 (1982).
- ²⁷A. Moritani, H. Sekiya, K. Taniguchi, C. Hamaguchi, J. Nakai, and R. Makabe, *Jpn. J. Appl. Phys.* **10**, 1410 (1971).
- ²⁸H. Arwin, D. E. Aspnes, and D. R. Rhiger, *J. Appl. Phys.* **54**, 7132 (1983).
- ²⁹D. T. F. Marple and H. Ehrenreich, *Phys. Rev. Lett.* **8**, 87 (1962).
- ³⁰J. N. Schulman and T. C. McGill, *Appl. Phys. Lett.* **34**, 663 (1979).
- ³¹T. F. Kuech and J. O. McCaldin, *J. Appl. Phys.* **53**, 3121 (1982).
- ³²Y. Guldner, G. Bastard, J. P. Vieren, M. Voos, J. P. Faurie, and A. Million, *Phys. Rev. Lett.* **51**, 907 (1983).
- ³³M. Cardona, *J. Phys. Chem. Solids* **24**, 1543 (1963).
- ³⁴M. L. Cohen and T. K. Bergstresser, *Phys. Rev.* **141**, 783 (1966).
- ³⁵F. Herman, R. L. Kortum, C. D. Kuglin, and J. L. Shay, in *Proceedings of the International Conference on II-VI Semiconducting Compounds, Brown University, 1967*, edited by D. G. Thomas (Benjamin, New York, 1967), p. 503.
- ³⁶S. Bloom and T. K. Bergstresser, *Phys. Status Solidi* **42**, 191 (1970).
- ³⁷M. L. Cohen and V. Heine, in *Solid State Physics*, edited by H. Ehrenreich, F. Seitz, and D. Turnbull (Academic, New York, 1970), Vol. 24, p. 37.
- ³⁸H. Overhof, *Phys. Status Solidi B* **43**, 221 (1971).
- ³⁹D. J. Chadi, J. P. Walter, M. L. Cohen, Y. Petroff, and M. Balkanski, *Phys. Rev. B* **5**, 3058 (1972).
- ⁴⁰S. Katsuki and M. Kanimune, *J. Phys. Soc. Jpn.* **31**, 415 (1971).
- ⁴¹H. Overhof, *Phys. Status Solidi* **45**, 315 (1971).
- ⁴²A. Kisiel and P. M. Lee, *J. Phys. F* **2**, 395 (1972).
- ⁴³D. J. Chadi and M. L. Cohen, *Phys. Rev. B* **7**, 692 (1973).
- ⁴⁴M. Podgórný and M. T. Czyzyk, *Solid State Commun.* **32**, 413 (1979).
- ⁴⁵A.-B. Chen and A. Sher, *Phys. Rev. B* **23**, 5360 (1981); **23**, 5645 (1981).
- ⁴⁶H. Ehrenreich and K. C. Haas, *J. Vac. Sci. Technol.* **21**, 133 (1982).
- ⁴⁷A.-B. Chen and A. Sher, *J. Vac. Sci. Technol.* **21**, 138 (1982).
- ⁴⁸K. C. Haas, H. Ehrenreich, and B. Velický, *Phys. Rev. B* **27**, 1088 (1983).
- ⁴⁹S. Wu, *Solid State Commun.* **48**, 747 (1983).
- ⁵⁰M. Cardona, *Phys. Rev.* **129**, 69 (1963).
- ⁵¹J. A. Van Vechten and T. K. Bergstresser, *Phys. Rev. B* **1**, 3351 (1970).
- ⁵²D. Stroud, *Phys. Rev. B* **5**, 3366 (1972).
- ⁵³D. J. Chadi, *Phys. Rev. B* **16**, 790 (1977).
- ⁵⁴O. Berolo, J. Woolley, and J. A. Van Vechten, *Phys. Rev. B* **8**, 3794 (1973).
- ⁵⁵V. Solsback and H. J. Richter, *Surf. Sci.* **97**, 191 (1980).
- ⁵⁶D. R. Rhiger and R. E. Kuaas, *J. Vac. Sci. Technol.* **21**, 168 (1982).
- ⁵⁷S. M. Kelso, D. E. Aspnes, M. A. Pollak, and R. E. Nahory, *Phys. Rev. B* **26**, 6669 (1982).
- ⁵⁸L. Viña and M. Cardona, this issue *Phys. Rev. B* **29**, 6739 (1984).
- ⁵⁹J. E. Rowe and D. E. Aspnes, *Phys. Rev. Lett.* **25**, 162 (1970).
- ⁶⁰R. Triboulet, *Rev. Phys. Appl.* **12**, 123 (1977).
- ⁶¹S. P. Kozyrev, L. K. Vodopyanov, and R. Triboulet, *Solid State Commun.* **45**, 383 (1983).
- ⁶²D. E. Aspnes, *Opt. Commun.* **8**, 222 (1973); D. E. Aspnes and A. A. Studna, *Appl. Opt.* **14**, 220 (1975).
- ⁶³D. E. Aspnes, *Appl. Phys. Lett.* **39**, 316 (1981).
- ⁶⁴N. M. Bashara and R. M. Azzam, in *Ellipsometry and Polarized Light* (North-Holland, Amsterdam, 1977).
- ⁶⁵D. E. Aspnes, *J. Opt. Soc. Am.* **64**, 812 (1974).
- ⁶⁶The importance of excitonic effects at the Λ transitions in CdTe was first suggested by Cardona and Harbeke [M. Cardona and G. Harbeke, *Phys. Rev. Lett.* **8**, 90 (1962)].
- ⁶⁷A. Savitzky and J. E. Gollay, *Anal. Chem.* **36**, 1627 (1974); J. Steinier, Y. Termonia, and J. Deltour, *Anal. Chem.* **44**, 1906 (1972).
- ⁶⁸G. Jordan-Engeln and F. Reutter, in *Numerische Mathematik für Ingenieure* (Bibliographisches Institut, Mannheim, 1973), Band 106, p. 66.
- ⁶⁹Y. Toyozawa, M. Inoue, T. Inui, M. Okazaki, and E. Hanamura, *J. Phys. Soc. Jpn. Suppl.* **21**, 133 (1967).
- ⁷⁰M. Cardona, *Modulation Spectroscopy*, Solid State Physics, edited by F. Seitz, D. Turnbull, and H. Ehrenreich (Academic, New York, 1966), Suppl. 11.
- ⁷¹D. E. Aspnes, *Phys. Rev. B* **12**, 2297 (1975).
- ⁷²A. G. Thompson, M. Cardona, K. L. Shaklee, and J. C. Woolley, *Phys. Rev.* **146**, 601 (1966).
- ⁷³S. S. Vishnubhatla, A. G. Thompson, and J. C. Woolley, *Can. J. Phys.* **45**, 2597 (1967).
- ⁷⁴V. A. Tyagai, O. V. Snitko, V. N. Bondarenko, N. I. Vitrikhovskii, V. B. Popov, and A. N. Krasiko, *Fiz. Tverd. Tela (Leningrad)* **16**, 1373 (1974) [*Sov. Phys.—Solid State* **16**, 885 (1974)].
- ⁷⁵E. W. Williams and V. Rehn, *Phys. Rev. Lett.* **27**, 798 (1968).
- ⁷⁶C. Alibert, G. Bordure, A. Laugier, and J. Chevalier, *Phys. Rev. B* **6**, 1301 (1972).
- ⁷⁷P. Parayanthal and F. Pollak, *Phys. Rev. B* **28**, 3632 (1983).
- ⁷⁸S. S. Vishnubhatla, B. Eyglunent, and J. C. Woolley, *Can. J. Phys.* **47**, 1661 (1969).
- ⁷⁹O. Berolo and J. C. Woolley, in *Proceedings of the Eleventh International Conference on the Physics of Semiconductors* (PWN-Polish Scientific, Warsaw, 1972), p. 1420.
- ⁸⁰J. A. Van Vechten, O. Berolo, and J. C. Woolley, *Phys. Rev. Lett.* **29**, 1400 (1972).
- ⁸¹P. M. Laufer, F. H. Pollak, R. E. Nahory, and M. A. Pollak, *Solid State Commun.* **36**, 419 (1980).
- ⁸²E. H. Perea, E. E. Méndez, and C. G. Fonstad, *Appl. Phys. Lett.* **36**, 978 (1980).
- ⁸³P. Parayanthal, C. S. Ro, F. H. Pollak, C. R. Stanley, G. W. Wicks, and L. F. Eastman, *Appl. Phys. Lett.* **43**, 109 (1983).
- ⁸⁴S. Antoci, E. Reguzzoni, and G. Samoggia, *Solid State Commun.* **9**, 1081 (1971).
- ⁸⁵O. Goede, L. John, and D. Hennig, *Phys. Status Solidi B* **89**, K183 (1978).
- ⁸⁶D. E. Aspnes, *Surf. Sci.* **135**, 284 (1983).
- ⁸⁷J. C. Phillips, *Phys. Rev. Lett.* **20**, 550 (1968).
- ⁸⁸R. L. Hengehold and C. R. Fraime, *Phys. Rev.* **174**, 808 (1968).
- ⁸⁹D. E. Aspnes, *Physica* **117&118B**, 359 (1983).
- ⁹⁰J. Humlíček, F. Lukeš, E. Schmidt, M. G. Kekoua, and E.

- Khoutsishvili, *Solid State Commun.* **47**, 387 (1983).
- ⁹¹W. Hanke and L. J. Sham, *Phys. Rev. B* **12**, 4501 (1975).
- ⁹²W. Hanke and L. J. Sham, *Phys. Rev. B* **21**, 4656 (1980).
- ⁹³H. J. Mattausch, W. Hanke, and G. Strinati, *Phys. Rev. B* **27**, 3735 (1983).
- ⁹⁴N. Meskini, H. J. Mattausch, and W. Hanke, *Solid State Commun.* **48**, 807 (1983).
- ⁹⁵W. Hanke, *Festkörperprobleme* **19**, 1 (1979).
- ⁹⁶J. C. Phillips, *Phys. Rev.* **136**, 1705 (1964).
- ⁹⁷C. B. Duke and B. Segall, *Phys. Rev. Lett.* **17**, 19 (1966).
- ⁹⁸B. Velický and J. Sak, *Phys. Status Solidi* **16**, 147 (1966).
- ⁹⁹E. O. Kane, *Phys. Rev.* **180**, 852 (1969).
- ¹⁰⁰Y. Petroff and M. Balkanski, *Phys. Rev. B* **3**, 3299 (1971).
- ¹⁰¹S. Antoci and G. F. Nardelli, *Phys. Rev. B* **6**, 1311 (1972).
- ¹⁰²G. Jungk, *Phys. Status Solidi B* **105**, 551 (1981).
- ¹⁰³G.-J. Jan and F. H. Pollak, *Sol. Energy Mater.* **8**, 241 (1982).
- ¹⁰⁴D. E. Aspnes, A. A. Studna, and E. Kinsbron, *Phys. Rev. B* **29**, 768 (1984).
- ¹⁰⁵D. J. Chadi, *Phys. Rev. B* **16**, 790 (1977).